

—Original—

# Assessment of liver fibrosis by ultrasound elastography and contrast-enhanced ultrasound: a randomized prospective animal study

Tingting QIU<sup>1)</sup>, Hong WANG<sup>1)</sup>, Jinzhen SONG<sup>1)</sup>, Wenwu LING<sup>1)</sup>, Yujun SHI<sup>2)</sup>, Gang GUO<sup>2)</sup>, and Yan LUO<sup>1)</sup>

<sup>1)</sup>Department of Ultrasound, West China Hospital Sichuan University, No.37 Guo Xue Xiang, Wu Hou District, Chengdu 610041, P.R. China

<sup>2)</sup>Research Institute of Pathology, West China Hospital Sichuan University, No.88 Ke Yuan South Road, Wu Hou District, Chengdu 610041, P.R. China

**Abstract:** This study aimed to assess liver fibrosis by contrast-enhanced ultrasound (CEUS) and point shear-wave elastography (pSWE) in rabbits and compare the performance of the two techniques. Eighty rabbits were divided into experimental (n=60) and control group (n=20). In the experimental group, liver fibrosis (F1–F4) was induced by subcutaneous injection of carbon tetrachloride. CEUS and pSWE of the liver was performed for the two groups at a 4-week interval for 40 weeks. The portal vein rise time (PV-RT), time to peak (PV-TTP), mean transit time (PV-MTT) and the maximum signal intensity (PV-I<sub>max</sub>) were analyzed with time-intensity curves (TICs). Liver stiffness value (LSV) was obtained through pSWE. Histologic examination of liver specimens of the rabbits was performed to evaluate the fibrosis stage. PV-RT, PV-TTP, PV-I<sub>max</sub> and LSV were significantly different among five liver fibrosis stages (F0–F4) ( $P < 0.01$ ). PV-I<sub>max</sub> and LSV displayed better diagnostic performance than PV-RT, PV-TTP, PV-MTT. For diagnosing  $\geq F1$  stage fibrosis, the area under the receiver operating characteristic curve (AUROC) of PV-I<sub>max</sub> was 0.870, which was similar to that of LSV 0.874 ( $P = 0.94$ ). For diagnosing  $\geq F2$ ,  $\geq F3$  and  $\geq F4$  stage fibrosis, the AUROC of PV-I<sub>max</sub> and LSV was 0.845 vs. 0.956 ( $P = 0.04$ ), 0.789 vs. 0.954 ( $P = 0.01$ ) and 0.707 vs. 0.933 ( $P = 0.03$ ). Both CEUS and pSWE had the potential to be complementary imaging tools in the evaluation of liver fibrosis. The performance of pSWE may be better than CEUS.

**Key words:** contrast-enhanced ultrasound, diagnostic performance, liver fibrosis, portal vein, ultrasound elastography

## Introduction

Liver fibrosis with different causes is a worldwide health threat with the risk of developing severe complications such as tumor, liver failure, esophageal variceal bleeding. Evaluation the degree of liver fibrosis, espe-

cially diagnosing early fibrosis is important for therapeutic management and prognosis [6, 11]. Although biopsy is the “gold standard”, sample bias and invasiveness limit its accuracy and repeated application within a clinical follow-up context [4, 20].

Ultrasound is a noninvasive and useful imaging tool

(Received 21 August 2017 / Accepted 10 October 2017 / Published online in J-STAGE 27 October 2017)

Address corresponding: Y. Luo, Department of Ultrasound, West China Hospital Sichuan University, No.37 Guo Xue Xiang, Wu Hou District, Chengdu 610041, P.R. China



This is an open-access article distributed under the terms of the Creative Commons Attribution Non-Commercial No Derivatives (by-nc-nd) License <<http://creativecommons.org/licenses/by-nc-nd/4.0/>>.

in examining the liver. But B-mode ultrasound and color Doppler are not sensitive for detecting early fibrosis. Ultrasound elastography and CEUS (contrast-enhanced ultrasound) have been considered potentially useful for assessing different stages of liver fibrosis from the perspective of stiffness change and hemodynamic alteration respectively [2, 7–8, 15]. However, the performance of ElastPQ (Elast Point Quantification, a type of point-shear wave elastography) in assessing different stages of fibrosis in animals was unclear. The hepatic transit time used for evaluation of liver fibrosis was also controversial [3, 21–22]. Ronot M *et al.* demonstrated that mean transit time was significantly increased in patients with intermediate fibrosis (F2 and F3) compared with those with minimal fibrosis (F1) [21]. But the study results of Staub F *et al.* showed that the transit time was significantly decreased ( $P < 0.0001$ ) in patients with severe fibrosis than those with normal liver or moderate fibrosis [22]. Furthermore, the performance of ultrasound elastography and CEUS for liver fibrosis assessment hasn't been compared before. Therefore, the present study aimed to assess different stages of liver fibrosis in animals by ElastPQ and CEUS respectively, and compare the performance of the two noninvasive ultrasound modalities.

---

## Materials and Methods

---

### *Animal model*

The use of experimental animals was approved by the Animal Ethics Committee of the West China Hospital, Sichuan University. All experiments were complied with the protocols and guidelines of the humane treatment of animals for research and teaching. Humane endpoints were established on the basis of the Guide for the Care and Use of Laboratory Animals published by the National Research Council (US) Committee for the Update of the Guide for the Care and Use of Laboratory Animals (8th edition. Washington (DC): National Academies Press (US); 2011.). From July, 2015 to October, 2016, a total of 80 New Zealand rabbits (mean age  $\pm$  SD = 120.5  $\pm$  20.5 days), each of which weighed about 2.5 kg at the beginning of this study, were enrolled and randomly divided into control group (n=20) and experimental group (n=60). For the animals in the experimental group, liver fibrosis was induced by subcutaneous injection of 0.3 ml/kg body weight of 50% carbon tetrachloride (CCl<sub>4</sub>) in olive oil as a vehicle, once a week. For the

control group, the animals received olive oil 0.3 ml/kg subcutaneous injection once a week.

### *Point shear-wave elastography examination of liver*

All ElastPQ examinations were performed with an iU22 ultrasound system (Royal Philips, the Netherlands) equipped with C5-1 (Curved 1–5 MHz) and L9-3 (Linear 3–9 MHz) transducer. The rabbits were anesthetized by intramuscular administration of 0.2 ml/kg zolazepam/tiletamine (Zoletil; Virbac Korea, Seoul, Korea) and 1–2 mg/kg xylazine hydrochloride (Rompun; Bayer Korea, Seoul, Korea). Following anesthesia, the rabbit was placed in supine position and its upper abdomen was prepared by shaving the hair for liver ultrasound scanning. The liver was initially examined with grey-scale ultrasound using C5-1 (Curved 1–5 MHz) probe. Liver lobe was displayed with subcostal scanning. With the transducer maintained in the same place and the liver in the selected section steadily displayed, the sonographic unit was then switched to ElastPQ mode. The size of the region of interest (ROI) box for Elast PQ was depth dependent with 0.5 cm  $\times$  1.5 cm at the depth of 4 cm. The penetration depth for all measurements ranged from 2 to 7 cm. The ROI was randomly put on the liver parenchyma for stiffness measurement, on the basis of avoiding large vessels and capsule (Fig. 1A). The IQR/M (ratio of inter quartile range to median) <30% was considered as successful measurement [15]. 10 measurements were carried out for each rabbit. The average successful measurement rate was about 70%. The measurement failure referred to stiffness value (LSV) equaled zero or IQR/M was over 30% and these results were discarded. All the pSWE examinations were carried out by one experienced (>5 years) sonographer who was blinded to the animal information and the pathologic results.

### *Contrast-enhanced ultrasound examination of liver*

All CEUS scanning were performed right after elastography examination with the same ultrasound system but the L9-3 probe (Linear 3–9 MHz). Because L9-3 probe had enough penetration with higher spatial resolution than C5-1 probe for rabbit liver scanning, whereas ElastPQ was only supported on C5-1 probe for this machine. Liver lobe was displayed with subcostal scanning. A section of the right portal vein without branch was displayed. With the transducer maintained in the same place and the liver in the selected section steadily dis-

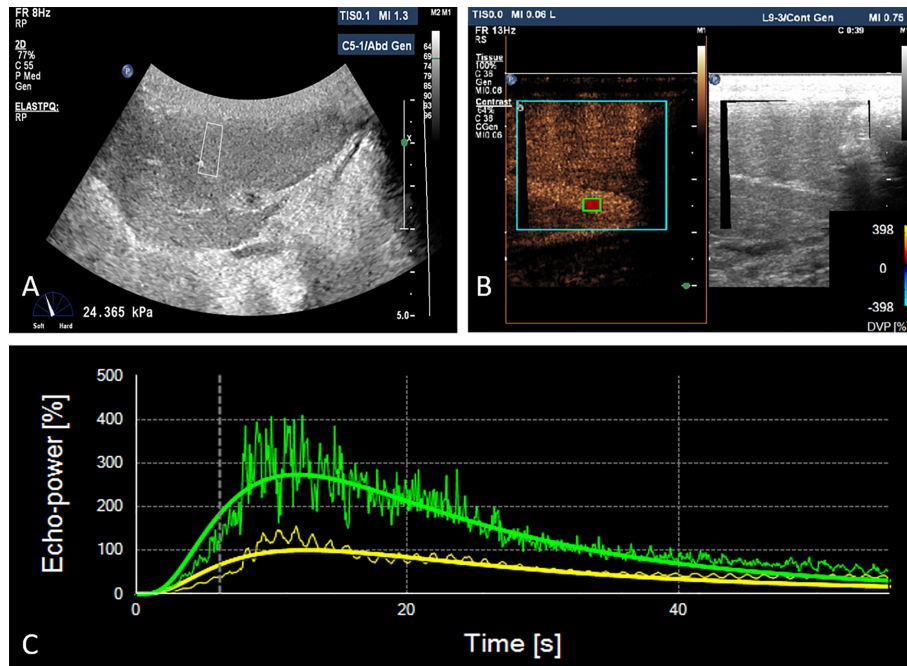


**Fig. 1.** A. *In vivo* stiffness measurement of the rabbit liver on the subcostal scan plane over B-mode ultrasound images. The white boxes represent ROI (region of interest) for stiffness measurement. B. A snapshot of the video clip of a contrast-enhanced ultrasound examination at 39 seconds after the injection of SonoVue. The sonogram on the right side is a grey-scale ultrasound, and the sonogram on the left side is in contrast mode. On the contrast mode image, the turquoise ROI included the right liver lobe on the subcostal scan plane, the green ROI was put on the portal vein. Motion compensation was applied automatically. C. Time-intensity curve (TIC) of portal vein (green line) and right liver lobe (yellow line).

played, the sonographic unit was then switched to dual-imaging contrast mode. The mechanical index was set at 0.06. The penetration depth for all measurements ranged from 2 to 7 cm. For grey-scale image, the overall gain was adjusted until the liver parenchyma was optimally visualized. For contrast mode image, the overall gain was set to display a complete anechoic image of the liver parenchyma for the basal phase. For both grey-scale and contrast modes, the focal zone was standardized to the bottom of the image. An ultrasound contrast agent (SonoVue, Bracco International, Amsterdam, Netherlands) at a dose of 0.2 ml/kg body weight was administered as a bolus into the auricular vein of the rabbit, followed by a 1.0 ml saline flush. Immediately after injection, continuously scanning of the liver was performed with the probe steadily maintained in the same place, and the images were recorded into a 60-second video clip, which was then stored in DICOM format for off-line analysis.

Time intensity curves (TIC) was generated from CEUS imaging clips on a PC-based workstation using

Sonoliver software (TomTec Imaging Systems, Munich, Germany). The right liver section and the right portal vein was outlined manually with caution as the region of interest for perfusion quantification (Figs. 1B and C). Perfusion parameters including portal vein rise time (PV-RT, s), time to peak (PV-TTP, s), mean transit time (PV-MTT, s) and the maximum signal intensity (PV-Imax, %) were analyzed automatically by the Sonoliver software. According to Sonoliver software, perfusion parameters RT refers to the time taken from 10% of  $f(x)$  ( $f(x)$  = best-fit function of echo power.) to the 90% of it. TTP stands for the time elapsed from time zero (arrival of contrast) to peak of  $f(x)$  ( $f(x)$  = best-fit function of echo power.). MTT represents the centre of gravity of  $f(x)$ , which corresponds to the time where as much contrast has passed before and after that instant. Imax is defined as maximum intensity (with respect to Imax of the reference ROI). Quality of fit between the echo-power signal and the perfusion model was over 85%. All the CEUS scanning and perfusion analysis were performed by one experienced (>10 years) ultrasound phy-

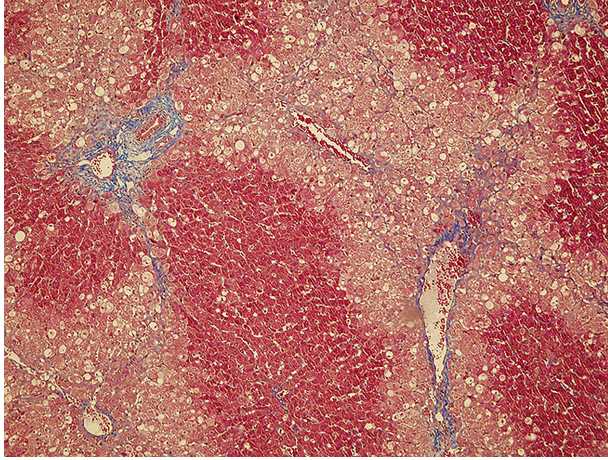


**Fig. 2.** Pathologic Masson trichrome staining ( $\times 100$ ) of liver tissue. Large areas of swollen and necrotic hepatocytes but no liver fibrosis.

sician who was blinded to the animal information, ElastPQ finding and pathologic results. The Kappa coefficient was 0.82 ( $P < 0.01$ ) for CEUS scanning and the ICC (intra-class correlation coefficient) was 0.76 ( $P < 0.01$ ) for perfusion analysis.

For both experimental and control groups, ElastPQ and CEUS examination were conducted in week 0 (as the baseline, before having any treatment), 4, 8, 12, ...4n ...until 40.

#### *Histological evaluation*

All rabbits were labeled with number (1, 2, 3...80). Every 4 weeks, 5 rabbits from experimental group and 2 rabbits from control group were randomly selected and sacrificed immediately after the ultrasound examination to obtain the liver specimen. Then these liver specimens were fixed with 10% formalin, and routinely embedded in paraffin. The tissue sections were stained with hematoxylin and eosin (H&E) and Masson. Pathological diagnosis was independently performed by two experienced ( $> 10$  years) pathologists, who were blinded to the animal information and the ultrasound findings. The final diagnosis was the consensus of the two pathologists. According to the METAVIR scoring system (modified according to the histopathological characters of  $\text{CCl}_4$ -induced liver lesion), liver fibrosis was staged on a scale of 0–4: F0: no fibrosis, F1: “centrilobular” fibrosis without septa, F2: “centrilobular” fibrosis and few septa, F3: numerous septa without cirrhosis, F4: cirrhosis.

**Table 1** Distribution of animals with different stages of fibrosis

Weeks	Animal Number (n)									
	Control					Study				
	Stages of fibrosis					Stages of fibrosis				
	F0	F1	F2	F3	F4	F0	F1	F2	F3	F4
4	2	0	0	0	0	0	4	1	0	0
8	2	0	0	0	0	0	3	2	0	0
12	2	0	0	0	0	0	2	3	0	0
16	2	0	0	0	0	0	1	4	0	0
20	2	0	0	0	0	0	0	4	1	0
24	2	0	0	0	0	0	0	3	2	0
28	2	0	0	0	0	0	0	0	4	1
32	2	0	0	0	0	0	0	0	3	2
36	2	0	0	0	0	0	0	0	2	3
40	2	0	0	0	0	0	0	0	0	5
SUM	20	0	0	0	0	0	10	17	12	11

#### *Statistical analysis*

Data were divided into groups according to the stage of liver fibrosis (F0–F4). A one-way analysis of variance (ANOVA) was used for the data complying to a normal distribution and homogeneity of variance. Tukey’s multiple comparison test was used for multiple comparisons. A Welch method was used if the variance showed heterogeneity, and a DunnettT3 method was used for multiple comparisons. The diagnostic performance of LSV and CEUS were compared through the area under the receiver operating characteristic curve (AUROC). An AUROC equal to 1.0 indicated the ideal parameter, while  $\text{AUROC} \leq 0.5$  indicated no diagnostic significance. Graphpad Prism 5.0 software package was used for statistical analysis.  $P < 0.05$  was considered to be significantly different.

## **Results**

#### *Pathologic results*

During the  $\text{CCl}_4$  treatment process, a total of 10 rabbits sacrificed in the experimental group due to acute liver failure ( $n=7$ ) (Fig. 2) and other undetermined causes ( $n=3$ ). Finally only 50 rabbits remained to be investigated in the experimental group. The distribution of animals with different stages of liver fibrosis over the 40 weeks of  $\text{CCl}_4$  treatment were illustrated in Table 1 and Fig. 3. In the experimental group, liver fibrosis was developed in the rabbits after 4 weeks of  $\text{CCl}_4$  treatment. The staging of liver fibrosis progressed from week 4 to week 40. Based on the staging category and biopsy find-

**Table 2** Comparison of liver stiffness value for liver fibrosis staging (median, range)

Liver fibrosis stage	Number of animals (n)	LSV (kPa, median, range)
F0	20	3.9 (1.9–8.5)
F1	10	5.0 (2.4–8.9)
F2	17	7.9* (5.2–12.3)
F3	12	12.8 <sup>†</sup> * (5.9–16.8)
F4	11	16.6 <sup>†</sup> * (9.8–29.5)
Summary	70	$P < 0.0001$

The results of Kruskal-Wallis test showed that  $P < 0.0001$  in liver stiffness value among different liver fibrotic stage. \* $P < 0.05$  compared with F0 stage; <sup>†</sup> $P < 0.05$  compared with F1 stage. LSV, liver stiffness value.

**Table 3** Comparison of CEUS hemodynamic indexes for liver fibrosis staging

Liver fibrosis stage	PV-MTT(s) (median, range)	PV-RT(s) (median, range)	PV-TTP(s) (median, range)	PV-Imax (%) (mean ± SD)
F0	28.3 (18.0–40.9)	9.5 (6.5–12.3)	11.4 (7.0–15.0)	454.5 ± 100.6
F1	34.7 (18.8–55.2)	11.5 (7.6–19.2)	11.5 (9.0–19.6)	358.6 ± 110.9
F2	36.7 (19.0–45.6)	10.0 (7.9–12.1)	11.1 (8.5–13.5)	274.0 ± 73.1*
F3	28.7 (16.0–47.8)	<sup>†</sup> *14.3 (7.1–20.6)	<sup>†</sup> *28.3 (8.3–39.7)	250.8 ± 102.2*
F4	31.4 (10.7–58.8)	11.6 (4.9–21.6)	13.7 (8.5–23.6)	260.3 ± 116.4*
Kruskal-Wallis / F	7.0	17.2	19.4	11.5
<i>P</i> value	0.136	0.0017	0.0007	<0.0001

The results of ANOVA and Kruskal-Wallis test showed that  $P > 0.05$  in PV-MTT of liver fibrosis among different stages;  $P < 0.05$  in PV-Imax, PV-RT and PV-TTP among liver fibrosis at different stages; \* $P < 0.05$  compared with F0 stage; <sup>†</sup> $P < 0.05$  compared with F2 stage. CEUS, contrast-enhanced ultrasound; PV, portal vein; Imax, maximum signal intensity; RT, rise time; TTP, time to peak; MTT, mean transit time.

ing, the 50 rabbits in the experimental group were classified to 4 groups: F1 (n=10), F2 (n=17), F3 (n=12), and F4 (n=11). Liver fibrosis wasn't found in any rabbit of the control group: F0 (n=20).

*Liver stiffness value at different stages of liver fibrosis*

Profiles for LSV (median, range, kPa) at different stages of liver fibrosis were illustrated in Table 2. The median LSV of F2 (7.9, 5.2–12.3 kPa), F3 (12.8, 5.9–16.8 kPa), and F4 (16.6, 9.8–29.5 kPa) stage were all significantly higher than that of the F0 (3.9, 1.9–8.5 kPa) stage ( $P < 0.001$ ). The median LSV of F3 and F4 stage was both significantly higher than that of the F1 (5.0, 2.4–8.9 kPa) stage ( $P < 0.01$ ).

*CEUS perfusion parameters at different stages of liver fibrosis*

In comparison of CEUS perfusion parameters as displayed by Table 3, PV-MTT were similar in each stage ( $P = 0.136$ ). PV-RT (median, range, s) of F3 (14.3, 7.1–20.6 s) was significantly higher than that of F0 (9.5, 6.5–12.3 s) ( $P < 0.001$ ) and F2 (10.0, 7.9–12.1 s) ( $P < 0.01$ ) stage. PV-TTP (median, range, s) of F3 (28.3, 8.3–39.7

s) was significantly higher than that of F0 (11.4, 7.0–15.0 s) ( $P < 0.0001$ ) and F2 (11.1, 8.5–13.5 s) ( $P < 0.001$ ) stage. PV-Imax (mean ± SD, %) of F2 (274.0 ± 73.1%), F3 (250.8 ± 102.2%) and F4 (260.3 ± 116.4%) stage was all significantly lower than that of the F0 (454.5 ± 100.6%) ( $P < 0.0001$ ) stage.

*Comparison of the performance of CEUS and LSV in assessment of liver fibrosis*

The diagnostic performance of CEUS and LSV was demonstrated by Fig. 4. For diagnosing ≥F1 stage fibrosis, the AUROC (95% confidence interval) of LSV and PV-Imax was 0.874 (0.790–0.959) and 0.870 (0.783–0.957) respectively with no significant difference ( $P = 0.94$ ). The AUROC of the other 3 parameters PV-RT, PV-TTP, PV-MTT was 0.722 (0.599–0.845), 0.676 (0.541–0.810) and 0.683 (0.553–0.813) respectively. For diagnosing ≥F2 stage fibrosis, LSV and PV-Imax illustrated an AUROC of 0.956 (0.914–0.997) and 0.845 (0.754–0.936) separately ( $P = 0.037$ ). The AUROC of PV-RT, PV-TTP and PV-MTT was 0.662 (0.528–0.797), 0.663 (0.529–0.797) and 0.586 (0.444–0.728) respectively. For diagnosing ≥F3 stage fibrosis, AUROC of

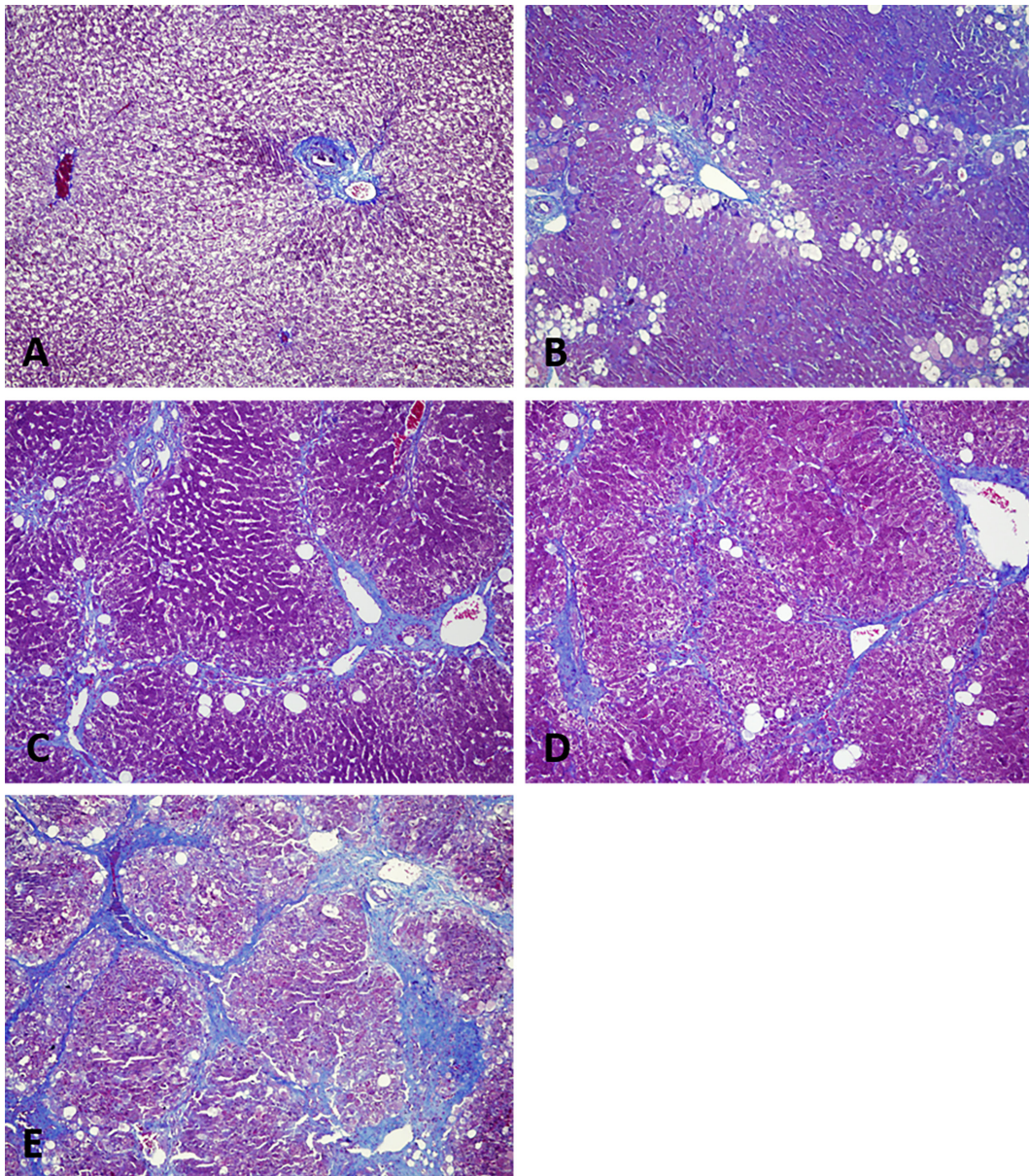


**Fig. 3.** Pathologic Masson trichrome staining ( $\times 100$ ) of different stages of liver fibrosis. F0: no fibrosis, F1: “centrilobular” fibrosis without septa, F2: “centrilobular” fibrosis and few septa, F3: numerous septa without cirrhosis, F4: cirrhosis.

PV-RT, PV-TTP, PV-Imax was 0.763 (0.622–0.904), 0.796 (0.662–0.930), 0.789 (0.669–0.908) respectively, while PV-MTT showed non-significant diagnostic accuracy (AUROC: 0.513,  $P=0.513$ ). LSV still displayed the highest AUROC of 0.954 (0.908–1.0). For diagnosing  $\geq$ F4 stage fibrosis, the AUROC of LSV was 0.933 (0.867–0.998), which was significantly higher than the other 4 CEUS perfusion parameters ( $P<0.004$ ). The AUROC of PV-RT, PV-TTP, PV-MTT and PV-Imax was

0.588 (0.370–0.806), 0.595 (0.411–0.778), 0.555 (0.327–0.782), 0.707 (0.524–0.890) respectively.

---

### Discussion

---

$\text{CCl}_4$  injection is a conventional and widely used approach to induce liver fibrosis in experimental animals. According to published data [5, 12, 16, 27], it took about 8–16 weeks to build liver cirrhosis in rabbits/dogs/pigs/

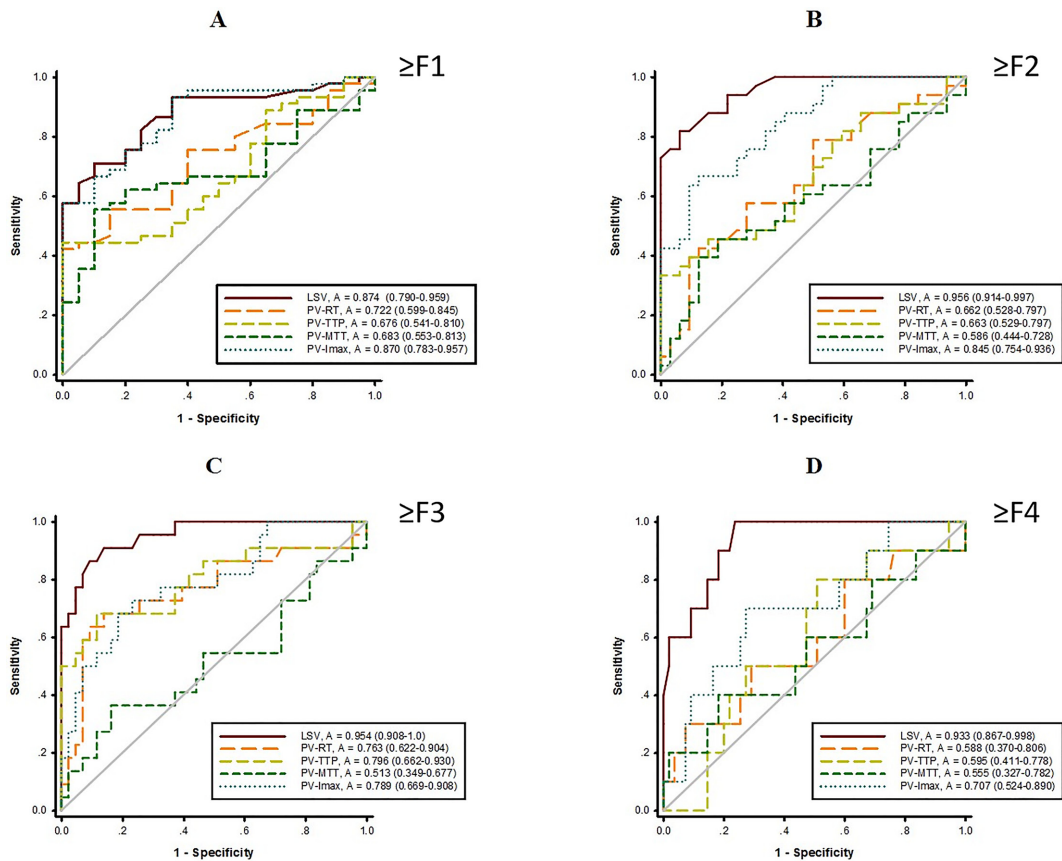


**Fig. 4.** Receiver operating characteristic curve of LSV (liver stiffness value), PV-RT (portal vein rise time), PV-TTP (portal vein time to peak), PV-MTT (portal vein mean transit time) and PV-Imax (portal vein maximum signal intensity) for diagnosing  $\geq F1$  (A),  $\geq F2$  (B),  $\geq F3$  (C),  $\geq F4$  (D) stages of liver fibrosis.

rats. And the dose was about 0.1–0.3 ml/kg of 40–60% CCl<sub>4</sub> oil mixture, twice a week, assisted by phenobarbital or alcohol drinks and/or high-fat and low-protein diet. This classic approach of inducing global liver fibrosis hasn't reported any tumor growth in this process so far. In this study, gradual observation of the development from liver fibrosis to cirrhosis was needed, thus less frequent dosing of CCl<sub>4</sub> (0.3 ml/kg, once a week) was applied and all rabbits were on a normal diet. After 40 weeks, METAVIR: F1–F4 liver fibrosis were produced. A mortality rate of about 16.7% (10/60) was observed during the process of CCl<sub>4</sub> treatment. A mortality rate of 0% to 60% has been reported before [5, 12, 16, 25].

Through literature review, a series of studies [3, 21, 22] looking into the relationship between hepatic transit time and liver fibrosis were performed with perfusion imaging (US, CT, MRI). The problem was the results were controversial [21, 22], which may due to different imaging techniques and different measurements of tran-

sit times. As for CEUS only, the reported accuracy and usefulness of hepatic vein transit time for liver fibrosis assessment varied across studies [1, 9, 13, 17]. Knowledge about the perfusion change of portal vein itself with liver fibrosis progression by CEUS was quite limited. Therefore, this study transferred the focus from hepatic vein to portal vein, and compared PV-RT, PV-TTP, PV-MTT and PV-Imax among different fibrosis stage. As displayed in Table 3, PV-RT and PV-TTP of F3 was significantly higher than that of F0 ( $P < 0.001$ ) and F2 ( $P < 0.01$ ) stage. PV-MTT were similar in each stage ( $P = 0.136$ ). In the development of liver fibrosis, various factors lead to deposit of collagen fibers in the Disse space. The deposition of collagen fibers can damage sinusoidal endothelial cells and induce micro-thrombosis [26]. These pathologic changes gradually lead to increase of the intra-hepatic vascular resistance, which may explain the gradually prolonged PV-RT and PV-TTP. However, portal vein/hepatic vein shunts and arterialisa-

tion of capillary beds in the liver can develop with the deterioration of fibrosis [23]. These factors on the other hand accelerated the passing rate of microbubbles, thus might keep the balance and may partly explain PV-RT and PV-TTP wasn't significantly prolonged in the F4 (cirrhosis) stage and PV-MTT appeared similar for F0–F4. PV-Imax of F2, F3 and F4 stage was all significantly lower than that of the F0 stage. PV-Imax decreased with increasing severity of hepatic fibrosis. According to CEUS theory, echo intensity is directly proportional to the amount of scatters within a certain imaging plane under certain incident frequency of ultrasound beam and scatter radius of the microbubbles. Based on tracer dilution principle, CEUS echo intensity is related to the concentration of microbubbles and also related to blood flow of tissue [24]. Therefore, under the condition of fixed device setting and microbubble concentration for performing CEUS in this study, the decrease of PV-Imax reflected the fact that portal vein blood flow was decreasing with liver fibrosis progression. This finding was in line with other studies investigating histopathologic and hemodynamic changes of liver fibrosis [14, 19, 21]. Among the 4 CEUS perfusion parameters, PV-Imax demonstrated the best performance for diagnosing different fibrosis stage ( $\geq F1, \geq F2, \geq F3, \geq F4$ ), especially for diagnosing non-advanced fibrosis stage ( $\geq F1, \geq F2$ ), as displayed in Fig. 4. The underlying reason for the better performance of PV-Imax for diagnosing non-advanced fibrosis needed to be further investigated. We speculated that this phenomenon may indicate the main decrease of portal vein blood flow may occur in the non-advanced fibrosis stage.

Ultrasound elastography is another non-invasive method to evaluate liver fibrosis by measuring liver stiffness. The reported application of ElastPQ in assessment of animal liver fibrosis was rare [25]. Our study results as displayed in Table 2 showed that LSV gradually elevated with liver fibrosis progression. However, there was no significant difference in LSV between intermediate stages of liver fibrosis, which was complied with published data [15]. As displayed in Fig. 4, LSV demonstrated a high accuracy of 0.874–0.956 for identifying each stage of liver fibrosis in this study. Similar findings were reported in the study of Lu *et al.* in patients with chronic hepatitis B [18]. Compared to the performance of CEUS for diagnosing liver fibrosis in this study, LSV was comparable to PV-Imax for diagnosing  $\geq F1$  stage, but better than PV-Imax for diagnosing the subsequent

fibrosis stage (F2–F4). Ultrasound elastography evaluates liver fibrosis from the “physical” perspective of stiffness. The quantified liver stiffness was thought to be related to the amount and microstructure of fiber components that change through the severity of fibrosis during disease progress [10, 18]. CEUS assesses liver fibrosis from the standpoint of hemodynamic changes during the course of liver fibrosis. The deposit of collagen fibers in the Disse space can partially induce the increase of the intra-hepatic vascular resistance and therefore influence portal vein perfusion as mentioned previously. Therefore, the accumulation of fibers in the liver in the early fibrosis stage ( $\geq F1$ ) may be the common main factor for inducing LSV and PV perfusion parameters alteration. However, in the subsequent stages, the portal vein/hepatic vein shunts and arterialisations of capillary beds in the liver gradually formed, which can greatly influence portal vein hemodynamics but may not be as influential to liver stiffness. This may partly explain why LSV was persistently elevated with fibrosis progression while portal vein perfusion parameters were not in this study.

There were some limitations of this study: (1) sample bias of liver biopsy (2) motion artifacts of CEUS and elastography, which may affect the accuracy of TICs and LSVs; (3) Chemical-induced liver fibrosis in animals may not be representative for various causes of liver fibrosis in humans. (4) Real time shear wave elastography (2D-SWE) with a larger and more flexible ROI, might be more accurate than pSWE for stiffness measurement and it will be investigated in the following study. (5) It would be better to monitor the influence of anaesthetic drugs (zolazepam/tiletamine combined with xylazine hydrochloride) to blood pressure and blood flow in this study.

In conclusion, both CEUS and pSWE had the potential to be complementary imaging tools in the evaluation of liver fibrosis. The accuracy of pSWE may be better than CEUS.

---

#### Conflict of Interest

---

The authors have no conflict of interest to this report.

---

#### Acknowledgement

---

This study was supported by National Natural Science Foundation, China (No. 81371556; 81671702; 81501488).

---

**References**


---

1. Abbattista, T., Ridolfi, F., Ciabattoni, E., Marini, F., Bendia, E., Brunelli, E., and Busilacchi, P. 2008. Diagnosis of liver cirrhosis by transit-time analysis at contrast-enhanced ultrasonography. *Radiol. Med. (Torino)* 113: 860–874. [[Medline](#)] [[CrossRef](#)]
2. Bamber, J., Cosgrove, D., Dietrich, C.F., Fromageau, J., Bojunga, J., Calliada, F., Cantisani, V., Correias, J.M., D’Onofrio, M., Drakonaki, E.E., Fink, M., Friedrich-Rust, M., Gilja, O.H., Havre, R.F., Jenssen, C., Klausner, A.S., Ohlinger, R., Saftoiu, A., Schaefer, F., Sporea, I., and Piscaglia, F. 2013. EFSUMB guidelines and recommendations on the clinical use of ultrasound elastography. Part 1: Basic principles and technology. *Ultraschall Med.* 34: 169–184. [[Medline](#)] [[CrossRef](#)]
3. Blomley, M.J.K., Lim, A.K., Harvey, C.J., Patel, N., Eckersley, R.J., Basilio, R., Heckemann, R., Urbank, A., Cosgrove, D.O., and Taylor-Robinson, S.D. 2003. Liver microbubble transit time compared with histology and Child-Pugh score in diffuse liver disease: a cross sectional study. *Gut* 52: 1188–1193. [[Medline](#)] [[CrossRef](#)]
4. Bravo, A.A., Sheth, S.G., and Chopra, S. 2001. Liver biopsy. *N. Engl. J. Med.* 344: 495–500. [[Medline](#)] [[CrossRef](#)]
5. Bravo, E., D’Amore, E., Ciaffoni, F., and Mammola, C.L. 2012. Evaluation of the spontaneous reversibility of carbon tetrachloride-induced liver cirrhosis in rabbits. *Lab. Anim.* 46: 122–128. [[Medline](#)] [[CrossRef](#)]
6. Chang, T.T., Liaw, Y.F., Wu, S.S., Schiff, E., Han, K.H., Lai, C.L., Safadi, R., Lee, S.S., Halota, W., Goodman, Z., Chi, Y.C., Zhang, H., Hinder, R., Iloeje, U., Beebe, S., and Kreter, B. 2010. Long-term entecavir therapy results in the reversal of fibrosis/cirrhosis and continued histological improvement in patients with chronic hepatitis B. *Hepatology* 52: 886–893. [[Medline](#)] [[CrossRef](#)]
7. Cosgrove, D., Piscaglia, F., Bamber, J., Bojunga, J., Correias, J.M., Gilja, O.H., Klausner, A.S., Sporea, I., Calliada, F., Cantisani, V., D’Onofrio, M., Drakonaki, E.E., Fink, M., Friedrich-Rust, M., Fromageau, J., Havre, R.F., Jenssen, C., Ohlinger, R., Saftoiu, A., Schaefer, F., Dietrich, C.F., EFSUMB 2013. EFSUMB guidelines and recommendations on the clinical use of ultrasound elastography. Part 2: Clinical applications. *Ultraschall Med.* 34: 238–253. [[Medline](#)] [[CrossRef](#)]
8. Claudon, M., Dietrich, C.F., Choi, B.I., Cosgrove, D.O., Kudo, M., Nolsøe, C.P., Piscaglia, F., Wilson, S.R., Barr, R.G., Chammas, M.C., Chaubal, N.G., Chen, M.H., Clevert, D.A., Correias, J.M., Ding, H., Forsberg, F., Fowlkes, J.B., Gibson, R.N., Goldberg, B.B., Lassau, N., Leen, E.L., Mattrey, R.F., Moriyasu, F., Solbiati, L., Weskott, H.P., Xu, H.X., World Federation for Ultrasound in Medicine., and European Federation of Societies for Ultrasound. 2013. Guidelines and Good Clinical Practice Recommendations for Contrast Enhanced Ultrasound (CEUS) in the Liver – Update 2012. *A WFUMB-EFSUMB Initiat Coop With Represent AFSUMB, AIUM, ASUM, FLAUS ICUS. Ultrasound Med. Biol.* 39: 187–210. [[Medline](#)] [[CrossRef](#)]
9. Cobbold, J.F.L., Patel, D., Fitzpatrick, J.A., Patel, N., Crossey, M.M., Abdalla, M.S., Goldin, R.D., Vennart, W., Thomas, H.C., and Taylor-Robinson, S.D. 2012. Accuracy and reliability of microbubble ultrasound measurements for the non-invasive assessment of hepatic fibrosis in chronic hepatitis C. *Hepatology* 42: 515–522. [[Medline](#)] [[CrossRef](#)]
10. Ding, H., Ma, J.J., Wang, W.P., Zeng, W.J., Jiang, T., Huang, B.J., and Chen, S.Y. 2015. Assessment of liver fibrosis: the relationship between point shear wave elastography and quantitative histological analysis. *J. Gastroenterol. Hepatol.* 30: 553–558. [[Medline](#)] [[CrossRef](#)]
11. Fattovich, G., Bortolotti, F., and Donato, F. 2008. Natural history of chronic hepatitis B: special emphasis on disease progression and prognostic factors. *J. Hepatol.* 48: 335–352. [[Medline](#)] [[CrossRef](#)]
12. Hall, P.D., Plummer, J.L., Ilesley, A.H., and Cousins, M.J. 1991. Hepatic fibrosis and cirrhosis after chronic administration of alcohol and “low-dose” carbon tetrachloride vapor in the rat. *Hepatology* 13: 815–819. [[Medline](#)] [[CrossRef](#)]
13. Kim, G., Shim, K.Y., and Baik, S.K. 2017. Diagnostic Accuracy of Hepatic Vein Arrival Time Performed with Contrast-Enhanced Ultrasonography for Cirrhosis: A Systematic Review and Meta-Analysis. *Gut Liver* 11: 93–101. [[Medline](#)] [[CrossRef](#)]
14. Kim, H., Booth, C.J., Pinus, A.B., Chen, P., Lee, A., Qiu, M., Whitlock, M., Murphy, P.S., and Constable, R.T. 2008. Induced hepatic fibrosis in rats: hepatic steatosis, macromolecule content, perfusion parameters, and their correlations—preliminary MR imaging in rats. *Radiology* 247: 696–705. [[Medline](#)] [[CrossRef](#)]
15. European Association for Study of Liver Asociacion Latinoamericana para el Estudio del Hígado 2015. EASL-ALEH Clinical Practice Guidelines: Non-invasive tests for evaluation of liver disease severity and prognosis. *J. Hepatol.* 63: 237–264. [[Medline](#)] [[CrossRef](#)]
16. Lv, M.D. and Huang, J.F. 1993. Establishment of liver cirrhosis through intraperitoneal injection of carbon tetrachloride and nutrient control in dogs (article in Chinese). *Chin. J. Exp. Surg.* 2: 56–57.
17. Lim, A.K.P., Taylor-Robinson, S.D., Patel, N., Eckersley, R.J., Goldin, R.D., Hamilton, G., Foster, G.R., Thomas, H.C., Cosgrove, D.O., and Blomley, M.J. 2005. Hepatic vein transit times using a microbubble agent can predict disease severity non-invasively in patients with hepatitis C. *Gut* 54: 128–133. [[Medline](#)] [[CrossRef](#)]
18. Lu, Q., Lu, C., Li, J., Ling, W., Qi, X., He, D., Liu, J., Wen, T., Wu, H., Zhu, H., and Luo, Y. 2016. Stiffness Value and Serum Biomarkers in Liver Fibrosis Staging: Study in Large Surgical Specimens in Patients with Chronic Hepatitis B. *Radiology* 280: 290–299. [[Medline](#)] [[CrossRef](#)]
19. Motosugi, U., Ichikawa, T., Sou, H., Morisaka, H., Sano, K., and Araki, T. 2012. Multi-organ perfusion CT in the abdomen using a 320-detector row CT scanner: preliminary results of perfusion changes in the liver, spleen, and pancreas of cirrhotic patients. *Eur. J. Radiol.* 81: 2533–2537. [[Medline](#)] [[CrossRef](#)]
20. Regev, A., Berho, M., Jeffers, L.J., Milikowski, C., Molina, E.G., Pyrsopoulos, N.T., Feng, Z.Z., Reddy, K.R., and

- Schiff, E.R. 2002. Sampling error and intraobserver variation in liver biopsy in patients with chronic HCV infection. *Am. J. Gastroenterol.* 97: 2614–2618. [[Medline](#)] [[CrossRef](#)]
21. Ronot, M., Asselah, T., Paradis, V., Michoux, N., Dorvillius, M., Baron, G., Marcellin, P., Van Beers, B.E., and Vilgrain, V. 2010. Liver fibrosis in chronic hepatitis C virus infection: differentiating minimal from intermediate fibrosis with perfusion CT. *Radiology* 256: 135–142. [[Medline](#)] [[CrossRef](#)]
  22. Staub, F., Tournoux-Facon, C., Roumy, J., Chaigneau, C., Morichaut-Beauchant, M., Levillain, P., Prevost, C., Aubé, C., Lebigot, J., Oberti, F., Galtier, J.B., Laumonier, H., Trillaud, H., Bernard, P.H., Blanc, J.F., Sironneau, S., Machet, F., Drouillard, J., de Ledinghen, V., Couzigou, P., Foucher, P., Castéra, L., Tranquard, F., Bacq, Y., d'Altéroche, L., Ingrand, P., and Tasu, J.P. 2009. Liver fibrosis staging with contrast-enhanced ultrasonography: prospective multicenter study compared with METAVIR scoring. *Eur. Radiol.* 19: 1991–1997. [[Medline](#)] [[CrossRef](#)]
  23. Sugimoto, H., Kaneko, T., Hirota, M., Tezel, E., and Nakao, A. 2002. Earlier hepatic vein transit-time measured by contrast ultrasonography reflects intrahepatic hemodynamic changes accompanying cirrhosis. *J. Hepatol.* 37: 578–583. [[Medline](#)] [[CrossRef](#)]
  24. Strouthos, C., Lampaskis, M., Sboros, V., McNeilly, A., and Averkiou, M. 2010. Indicator dilution models for the quantification of microvascular blood flow with bolus administration of ultrasound contrast agents. *IEEE Trans. Ultrason. Ferroelectr. Freq. Control* 57: 1296–1310. [[Medline](#)] [[CrossRef](#)]
  25. Wang, M.J., Ling, W.W., Wang, H., Meng, L.W., Cai, H., and Peng, B. 2016. Non-invasive evaluation of liver stiffness after splenectomy in rabbits with CCl<sub>4</sub>-induced liver fibrosis. *World J. Gastroenterol.* 22: 10166–10179. [[Medline](#)] [[CrossRef](#)]
  26. Wanless, I.R., Wong, F., Blendis, L.M., Greig, P., Heathcote, E.J., and Levy, G. 1995. Hepatic and portal vein thrombosis in cirrhosis: possible role in development of parenchymal extinction and portal hypertension. *Hepatology* 21: 1238–1247. [[Medline](#)]
  27. Zhang, J.J., Meng, X.K., Dong, C., Qiao, J.L., Zhang, R.F., Yue, G.Q., and Zhong, H.Y. 2009. Development of a new animal model of liver cirrhosis in swine. *Eur. Surg. Res.* 42: 35–39. [[Medline](#)] [[CrossRef](#)]